



Field and Satellite Images-Based Investigation of Rivers Morphological Aspects

Ala Hassan Nama^{1, 2*} , Ali Sadiq Abbas¹, Jaafar S. Maatooq¹ 

¹ Civil Engineering Department, University of Technology-Iraq, Baghdad, Iraq.

² Department of Water Resources Engineering, University of Baghdad, Baghdad, Iraq.

Received 08 April 2022; Revised 18 June 2022; Accepted 26 June 2022; Published 01 July 2022

Abstract

Worldwide and especially in less developed regions, process-based evaluations and/or geomorphological information on large-scale rivers are still scarce. Such investigation become of urgent need due to the climate change and expected occurrence of extreme floods and drought which may threaten the safety of nearby and downstream cities, especially in regions that are highly sensitive and affected by climatic changes. The Tigris River, in Iraq, is one such river that has undergone significant alteration to its flow and morphologic aspects due to climate change and the construction of many dams. However, morphology and its change for many reaches of this river are still uninvestigated. To this end, field and satellite-based investigations into the morphology of a reach located between Makhool District and Tikrit City have been conducted. In addition to the cross-sectional survey-based determination of the reach geometrical aspects, a sinuosity indices-based evaluation of the reach planform was implemented, utilizing a satellite indices-based approach. Furthermore, the characteristics of bed material were identified through field sampling. Investigation results show that the reach has a steep bed slope and many islands of low altitude with an elongated shape. The reach has a mild sinuosity with alternating bars. The dominant particle sizes of the bed material are coarse and medium gravel with a dominant particle shape of disc particles. Moreover, the satellite-based change detection indicated the fading out and disappearance of some secondary channels, the growth of many islands, and the movement of some bends downstream. The percentage of changing parts for the period 1975–2021 is 14%. Most of this change, 11%, occurred after the construction of the Mosul Dam. This reveals the sensitivity of reach morphology to flow change due to the construction of dams. The conducted fieldwork and the applied methodology contribute to supporting efforts to add knowledge worldwide about uninvestigated rivers.

Keywords: Planform; Morphology; Satellite-Vased Indices Sinuosity.

1. Introduction

The morphological aspects of rivers are key components in the management of river basins. Evaluation of these aspects, such as river planform, the land cover of flood plains, and geometry, has great significance for river hydrodynamics and ecosystem functions [1]. Assessment of these aspects needs detailed spatial hydrological and topographical information. In recent decades, global climate changes have been observed [2]. However, little work has been done on the observed impacts of climate change and the impact of dams on downstream flow and sediment regimes in rivers, especially in large river systems [3, 4]. The majority of studies in such fields focus on identifying the dominant impacts on river planforms such as human land use, flow variation, flood frequency, sediment concentration, and precipitation [5-7]. Efficient monitoring and forecasting of floods as well as identification of

* Corresponding author: bce.19.02@grad.uotechnology.edu.iq

 <http://dx.doi.org/10.28991/CEJ-2022-08-07-03>



© 2022 by the authors. Licensee C.E.J, Tehran, Iran. This article is an open access article distributed under the terms and conditions of the Creative Commons Attribution (CC-BY) license (<http://creativecommons.org/licenses/by/4.0/>).

hydraulic characteristics, which in turn are necessary for achieving sustainable management of water resources, depend on the accurate delineation and mapping of the river system, planform, land cover, and flow rates. Recently, measurement of riverbank and channel shifting has been made using satellite-based approaches which essentially depend on satellite-based indices such as Normalized Difference Vegetation Index (NDVI) and Normalized Difference Water Index (NDWI) with the aid of the Geographic Information System (GIS). Such approaches provide large spatial and multi-temporal coverage with a direct, integrated, and synoptic view of vast areas. The morphological parameters such as sinuosity index, channel surface area, channel erosion/deposition, channel centerline, and channel width have been utilized in various studies to examine the river morphology with the help of satellite images. In addition to the progress made in terms of accuracy and resolution techniques increases the potential to get highly accurate large-scale maps reveals the river platform and land cover [8, 9].

The nature of the riverbed has a significant influence on the river's morphological and hydrodynamic characteristics [10]. Bed material characteristics are an important input in commonly applied theories and simulation models in the computations concerning river engineering and river morphology. Conventional bed material sampling methods, in a lot of cases, are time-consuming and expensive, especially when dealing with large rivers of inhomogeneous bed composition [11]. Therefore, in many rivers worldwide there are some uninvestigated reaches in terms of bed material. This lack of data constitutes a major obstacle to conducting comprehensive studies on the morphological characteristics of these rivers and evaluating changes in these characteristics. Thus, plans and decisions taken to achieve the river's function in normal conditions and to control the risks of extreme events will be unreliable because of they relied on inaccurate data.

Tigris River, in Iraq, is one of the longest rivers in the west of Asia. Over the last half-century, Great changes have occurred in the flows of this in terms of the amount and time of these flows due to climatic changes, the construction of many dams by Turkey, Iran, and Iraq, and a rapid increase in water demand [12]. Along this river, the change in morphology of many reaches is still uninvestigated. Makhool-Tikrit Reach, which is 88.2 km in length and extended from the Makhool mountains series to Tikrit City, 180 km north of Baghdad City, is one of the uninvestigated reaches in terms of morphological aspects. In 2021, the Iraqi Ministry of Water Resources (*IMoWR*) started to construct a proposed dam, named Makhool Dam, upstream of this reach. Expected morphological and flow changes indicate the need for a detailed study of the morphological characteristics for this reach.

Many researchers studied the morphological aspects of various reaches of the Tigris River such as Mosul, Baghdad, Kut, and Amaraa [13-22]. Most of these works are restricted to the geometry and/or the bed material of these reaches. The commonly applied methodology in these studies was the cross-sectional survey and/or bed materials sampling and laboratory analysis. All of these studies lacked the use of remote sensing techniques and focused on field and laboratory works. Globally, the researchers have moved away from using field works to avoid wasting time and resources and started using satellite data for morphological analysis such as [23-26]. Worldwide, the satellite data was included in most of the morphological aspects studies such as river planform morphology, variation in vegetation cover for the banks and main river islands, analysis and quantify the bank movements and width changes, migration rate of river banks, island growth, information about the active channel surface subdivision in water, vegetation and gravel coverage classes along the channel centerline, braiding and sinuosity indices, channel adjustments and alteration of sediment fluxes and interpret changes in channel conveyance. Many scholars used satellite data and GIS to assess the morphological changes in different places such as sand bed river flows in India and Bangladesh, five gravel-bed rivers in the north and north-eastern Italy, the Karkheh River in Iran, many rivers in Albania, and the Indus River in Pakistan [1, 4, 8, 27-30].

Sinuosity in alluvial rivers is proved to be a very significant index as it quantifies the amount to which a river loses its integrity. Sinuosity indices are used by researchers for multipurpose such as investigation of structural control of river basins [31], studying the role of tectonic activities in shaping the river basin [32] identifying the climatic signatures in river incision [33], and the alteration by human interventions [34].

The Middle East region, including Iraq, witnessed a significant decrease in its water resources [35]. One of the most important approaches that can be used to conserve surface water sustainability in Iraq is studying the spatiotemporal change in the morphological aspects of the Tigris River, which is considered the most influential factor in the conveyance capacity of the river. Many studies have reviewed the morphological aspects of the Tigris River in Iraq, but mostly they were limited to some reaches. Despite the importance of remaining reaches in terms of hydraulic and morphologic aspects of the river, extensive studies in this aspect are lacking. Othman and Deguan (2004) [13] conducted field and laboratory investigations for the characteristics of the Tigris River bed material downstream of Mosel Dam. Thereafter, Badowi et al. (2019) [36] investigated the physical and chemical characteristics of bed sediment for the flood plain of the Tigris River within Tikrit City. Also, Al-Ansari et al. (2015) [16] investigated the bed material of the Tigris River along a reach of 18 km within Baghdad City. In addition, the bed material of Tigris River 67 km downstream of the Kut Barrage was studied by Shamkhi and Attab (2019) [18]. Furthermore, Ismaeel et al. (2021) [22] studied the bed material of the Tigris River downstream Al-Amarah Barrage. A comprehensive review

of the previous works shows that there is a severe deficiency in the study of the morphological characteristics of some reaches of the Tigris River, such as the Makhool-Tikrit Reach.

Recently, after drought periods of 2 to 3 years, severe flood waves have occurred in the Tigris River due to the flow of large quantities of water from the tributaries of the Tigris River, in addition to the water released from the Mosul Dam. Consequently, these flood waves flow in the Tigris River through Makhool-Tikrit Reach down to the Samarra Barrage without any control. Thus, these floods threaten the areas adjacent to this reach and then Baghdad City, which is located downstream of the Samarra Barrage. Therefore, it is vitally important to conduct a detailed investigation of the morphological characteristics of this reach. Worldwide and especially in less developed regions, process-based evaluations and/or geomorphological information of large scales river systems are still scarce. This scarcity is caused by the lack of necessary sources for collecting, storing, and processing, and interpreting hydro-morphological data. Hence, such investigation becomes of urgent need due to the climate change and expected occurrence of extreme floods and drought which may threaten the safety of nearby and downstream cities, especially in regions that are highly sensitive and affected by climatic changes, where Iraq is one of these areas. This paper aims to investigate and evaluate the geomorphological aspects of the Makhool-Tikrit Reach of the Tigris River.

2. Materials and Methods

2.1. Study Area

Tigris River is one of the longest rivers in West Asia, it has a total length of 1850 km. The river originates in Turkey and augmented by several rivers in Iraq, the most important are Khabur, Great Zab, Lesser Zab, Al Adhaim, and Diyala River. Most of them have their origin in Turkey and Iran [37]. On the main Tigris River within Iraq, the Mosul Dam was constructed in 1986 with a reservoir capacity of 11.11 km³ and the Makhool Dam is under construction since 2021. The latter is located on the Tigris River at 30 km northwest of Baiji Town and about 15 km downstream from the junction of the Lesser Zab River with the Tigris River (Figure 1). The reservoir of the dam will extend to Sharqat Vicinity, with a maximum water level of 150 m.a.s.l., and a maximum storage volume of 2.9 km³ [38]. In addition, several dams were constructed on the tributaries of the Tigris River. These dams are; Dokan, constructed in 1959 on Lesser Zab River with a reservoir capacity of 6.8 km³, Darbandikhan, constructed in 1961 on Diyala River with a reservoir capacity of 2.8 km³, Hemrin, constructed in 1981 on Diyala River with a reservoir capacity of 2.4 km³, and Adhaim, constructed in 1999 on Adhaim River with a reservoir capacity 1.5 km³ [39].

At Samarra City, a barrage was constructed in 1956 to control flood waves by diverting excess water from the Tigris River to Tharthar Lake and generating electricity. The bed materials of the Tigris River changes along the river from a dominant very coarse gravel of 74% in the surface layer within Mosul City to a major component of fine sand (finer than 0.3mm diameter) within Baghdad City and dominant composition of 40.30% silt and 41.29% clay within Kut and Amarah cities. The maximum (minimum) concentration of suspended sediments in Mosul, Baghdad, Kut, and Amarah is about 630 (30), 1100 (190), 1319 (135), and 1319 ppm (132 ppm), respectively. The sharp decrease in discharges and construction of hydraulic structures caused the emergence and growth of many bars and islands along the river.

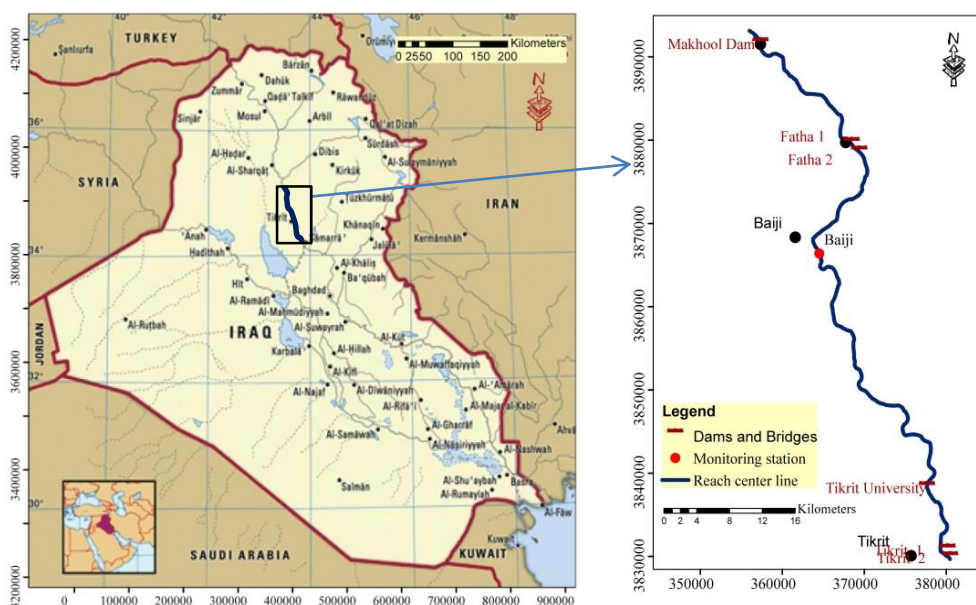


Figure 1. Location of Makhool-Tikrit Reach of Tigris River

In 2021, IMoWR starts construction of the Makhool Dam, in the north of Salahaldin Province, Iraq. The Makhool-Tikrit Reach of the Tigris River extends from the Makhool Dam to Tikrit City, 180 km north of Baghdad City (Figure 1). This river reach is affected by the change in the flow rates, debris from bridges damaged through the military operation from 2014 to 2016, which causes extensive changes in morphology and hydraulic performance of the river. Within this reach, a large number of growing islands can be noticed with some bends down to Tikrit City.

2.2. Methodology

In this paper, the followed methodology to investigate the morphological aspects of the considered river reach is summarized in the schematic diagram shown in Figure 2. This methodology is mainly based on determining the river planform measures by using satellite based-indices, field topographical survey, and field hydraulic measurements as well as specifying the bed material of the river reach. Subsequently, the present morphological aspect of the reach and the change in reach planform were evaluated for the period 1975-2021. As there were no previous studies that included topographic survey, hydraulic measurements, and land cover investigations to study the planform and morphological aspects of this reach. In addition, in Iraq, it is the first study that applied the satellite-based indices to investigate the planform of this reach, therefore, the obtained results could not compare with other previously studied. Even on a global scale, the morphological aspects of the studied rivers have their peculiarity and differ from the considered river reach. Hence, this paper will be a basis for monitoring future changes in these aspects.

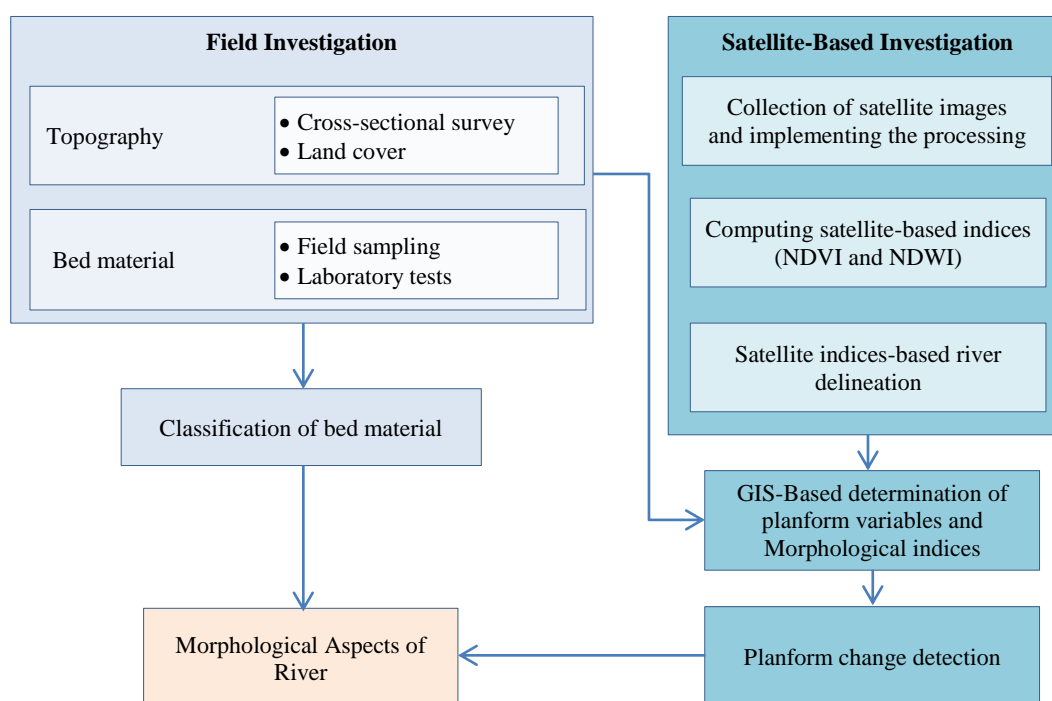


Figure 2. Schematic diagram of the methodology

2.3. Determination of River Planform

Planform is a commonly studied aspect of river systems, and planform change is usually measured through a comparison of historical sources (typical maps, aerial photographs, and satellite images), although this approach can only detect relatively large-scale changes. Long-term analysis of fluvial planforms may reveal whether fluvial system behavior is in dynamic equilibrium or transitioning to a new state [40]. Such knowledge is essential for developing predictive river bank erosion models, understanding local riparian communities, and informing appropriate land-use planning [41]. Compared with manual comparison methods, remote sensing and GIS analysis are advantageous in flexibility to utilize multi-modal datasets, processing speed, and uncertainty treatment [42].

The main focus of researchers has been the identification of the thresholds between straight, meandering, and braided reaches, the planform properties of meanders, the relations between their geometric variables, and meander behavior with geologic, hydrologic, and geomorphic controls. Whereas one of the main indices is river sinuosity, it was defined as the degree to which a river channel departs from a straight line towards a meandering (sine curve shape) planform [43–46]. A variety of sinuosity indices were proposed. In 1968, Mueller enumerated and explained river sinuosity indices as Hydraulic Sinuosity Index (HSI), Topographic Sinuosity Index (TSI), and Standard Sinuosity Index (SSI). These indices are mainly based on the Channel Index (CI) and Valley Index (VI), which in turn are a function of the Channel Length (CL) as measured along the Thalweg line, the Airline Length (AL) between the two

endpoints of the reach and the Valley Length (VL), which is a line everywhere midway between the base of the valley walls [47]. Details of how can calculate these sinuosity indices are found in Khan et al. (2018) [3]. Charlton (2007) [48] classify the sinuosity based on the CI into straight ($CI < 1.1$), sinuous ($1.1 < CI < 1.5$), and meandering ($CI > 1.5$).

Another index used in river form description is the braiding index. In general, the braiding index has been based on one of three characteristics; bar dimensions and frequency, the number of channels in the network, and the total channel length in a given river length. Based on these characteristics, different formulas have been presented in the literature to calculate the braiding index, such as those proposed by Brice (1964) [49], Rust (1977) [50], Germanoski and Schumm (1993) [51] and Friend and Sinha (1993) [52]. All formulas depend, for index calculation, on the length of all the islands and/or bars in the reach, the length of the reach measured midway between the banks of the channel belt, the total number of bars, the sum of the braid lengths in a reach between channel thalweg divergences and confluences, and the main of the meander wavelengths in a reach of the channel belt.

In this paper, the Braiding Ratio Index (BRI), which is the ratio of the total area of the islands and bars (A_b) to the total channel area (A_c) [53], and the Modified Braid Index (MBI), which proposed by Germanoski and Schumm (1993) [51] based on the originally devised braid index (BI_B) by Brice (1964) [49] was used. This index takes into account the number of bars and islands (N_b) in addition to the VL, and the sum of bars and island length (L_b). According to Sarma and Acharjee (2018) [54], a river is braided when it has a braiding index of more than 1.5, whereas, it is sinuous with alternating bars if the braiding index is less than 1.5 and near 1.0, otherwise, it is wandering [55].

2.3.1. Satellite-Based Investigation

The satellite-based method can be effectively utilized to extract the data used for obtaining the morphological indexes [4, 18, 29, 30]. Delineation of the river region to specify the river boundaries, flood plains, main channel, island, bars, and other features within the river is the first step in determining the morphological aspect of the river. To this end, satellite-based indices such as Normalized Difference Vegetation Index (NDVI) and Normalized Difference Water Index (NDWI) were used. The NDVI quantifies vegetation by measuring the difference between near-infrared, which vegetation strongly reflects, and red light, which vegetation absorbs, which has been proposed by Huang et al. (2021) [56]. Whereas, NDWI is a radiometric index that exploits a typical absorption/reflection pattern to delineate open water features and enhance their presence in remotely-sensed digital imagery. This index was proposed by McFeeters (1996) [57]. The first formula depends on the near-infrared and red spectral band, while the second formula depends on the green band with near-infrared.

The NDVI increases with increasing green biomass with a typical range of -1 to $+1$. However, it is about -0.1 for non-vegetated surfaces and 0.9 for dense green vegetation canopies [58]. In Iraq, Partow and Jaquet (2006) [59] studied the NDVI thresholds and showed that values greater than 0.125 represented vegetative cover, sparse vegetation was found to correspond to NDVI values between 0.125 and 0.25 , medium-density vegetation was associated with NDVI values between 0.25 and 0.5 , while dense vegetation was found to occur in areas with NDVI values over 0.5 . In this paper, the same thresholds were adopted and verified according to a set of in situ training points. On the other hand, regions covered with (deep) water were identified based on their NDWI, with regions having NDWI greater than zero defined as regions with open water [60]. For using the satellite-derived NDWI to delineate surface water features, the recommended procedure by Ji et al. (2009) [61] was followed.

The Arc GIS, ArcMap-10.8 was used to implement the land cover classification process and determine the values of morphological indexes variables. The images of Landsat 1–5 MSS (1975, 1984, and 1988), Landsat 4–5 TM (1995 and 2000), Landsat 7 ETM (2005 and 2010), Landsat 8 OLI/TIRS (2015, 2019, and 2021) for the wet (represented by April) and dry (represented by September, except for 1975 where it was for July, because of cloud cover problems) seasons of each year were downloaded from the USGS website (<http://earthexplorer.usgs.gov/>) to perform the planform investigation. These years were selected to represent the situation of the river before the construction of Mosul Dam in 1986 and to investigate the effect of water shortage due to climate change on the morphology of this reach until the year 2021. However, the Dukan Dam was constructed on Lesser Zab in 1956, which is too old to regard its effects now. This satellite-based investigation was supported and verified by results of the field topographical survey conducted in Sept. 2020 and Shuttle Radar Topographic Mission (SRTM) Digital Elevation Model (DEM) with a spatial resolution of 90 m, downloaded from the USGS website (<http://earthexplorer.usgs.gov/>).

2.3.2. Topographical and Hydraulic Data

To study the geometry of the main channel and flood plains as well as features of land surfaces of the river, a topographical survey was conducted in Sept 2021, with the assistance and support of IMoWR. This survey involved a cross-sectional survey for 15 Cross-Sections (CSs) and locations of bridges and other main features (Figure 1). Furthermore, a set of measurements for the 2-D flow velocity, discharge, and water depth at the same 15 CSs were

conducted in Sept 2021 by using Aquatic Doppler Current Profiler (ADCP). In addition, a monthly measurement for these flow parameters was conducted at the first CS, at the location of the proposed Makhool Dam, on 9 Sept 2021, 21 Oct 2021, 18 Nov 2021, 29 Dec 2021, 27 Jan 2022, and 24 Feb 2022. However, to investigate the change in river planform, the recorded (available) discharge (Q) and Water Surface Elevation (WSE) at Baiji Hydrological Station, Figure 1, for the period 1975-2021, listed in Table 1, was used to specify the year of low and high discharge and those have the same discharge [62].

Table 1. Average monthly Q and WSE at Baiji Hydrological Station (Based on IMoWR 1985, unpublished report; IMoWR 2021, unpublished data)

Year	Month	Q (m ³ /s)	WSE (m.a.s.l.)
1975	April	2356	104.6
	July	435	102.6
1984	April	2000	104.4
	September	450	102.7
1988	April	9917	107.2
	September	1007	103.51
1994	April	3000	105.1
	September	500	102.9
2000	April	1000	103.5
	September	400	102.5
2005	April	1010	103.5
	September	523	102.9
2010	April	3320	105.2
	September	213	102.4
2015	April	1500	104.1
	September	400	102.5
2019	April	10533	107.4
	September	902.2	103.4
2021	April	738	103.1
	September	437	102.7

2.4. Determination of Bed Material

To study the physical properties of the bed material for the Makhool-Tikrit Reach, field sampling was carried out in Sept 2021. Guidelines presented by Diplas & Sutherland (1988) [63] were followed to specify sampling locations, sample size, and sampling method. At the same location of the surveyed 15 CSs in Sept 2021, along the Makhool-Tikrit Reach, three samples of surface and sub-surface layer were collected at distances 1/4, 1/2, and 3/4 of the average width of each CS following the areal method for sampling. This method gives grain size information from a small area of sampling [64].

A hand tool excavator was used to collect the particles of the surface layer, and then a subsurface sample was taken by using a Van Veen grab of size 3.14 L. Following the Fripp & Diplas (1993) [64] method, Van Veen grab was used in sampling the surface layer in some locations where the surface layer consists of fine grain sizes particles. More than 100 particles were collected from the three locations in each CSs for surface layer sampling. The thickness of the surface layer is approximately equal to the diameter of the largest particle [65]. Grain size analysis was carried out, in the laboratory of soil physics at the University of Baghdad, Iraq, to determine the grain size distribution of the river bed materials. The shape of particles is specified based on Zingg's classification [66].

3. Results and Discussion

3.1. Field Investigation

The surveyed 15 CSs (Figure 3) showed a significant variation in width, depth, and location of the Thalweg line as well as severe change in bed level of the main channel can be noticed in CSs along the river reach. The river bed level

changed from 100 m.a.s.l. at the location of Makhool Dam to 70 m.a.s.l. in Tikrit City. River width is less than 250 m in CS2, CS11, CS12, and CS15 and increased to more than 700 m in CS1, CS4, and CS7. Large islands are growing in these wide CSs. Some of these CSs have high banks with a steep lateral slope on both sides such as CS4, CS8, and CS14. Thus, these CSs safely control and convey the flood wave and prevent the flood risk. However, other CSs characterize by extreme flatness which exposes the regions near these CSs to flood risk. At some reaches the river braided into two or three deep channels, this is clear at CS4 where the river course braided into two channels for about 1.5 km and at the reach extended between CSs 7 to 9 where it braided into three channels.

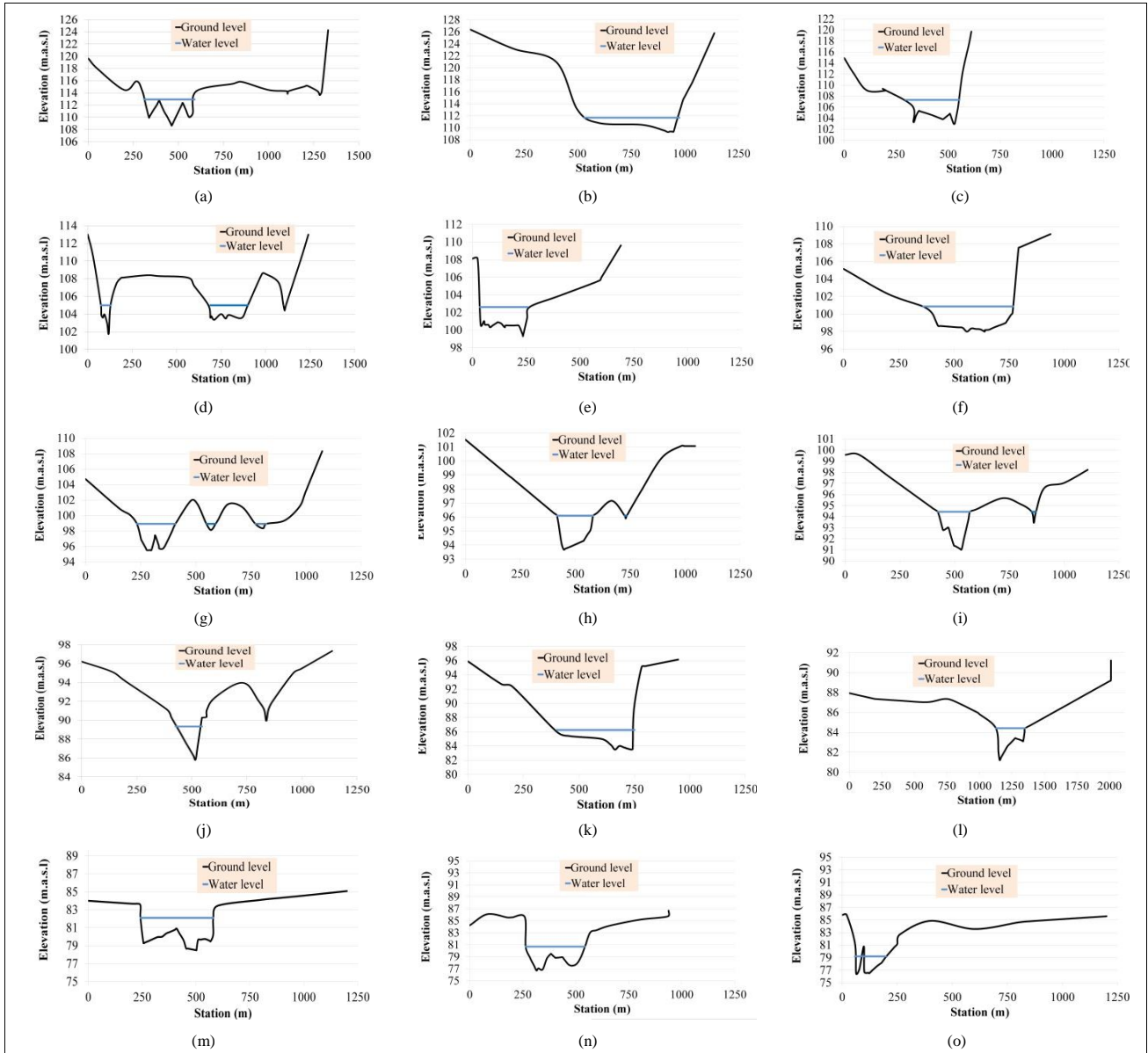


Figure 3. Surveyed cross-sections (CSs): (a)-(o) for CS1 to CS15, respectively

Profiles of the river bed (minimum bed elevation at each CS), measured Q, and WSE at these CSs are shown in Figure 4. In general, the bed elevation of the reach has a steep longitudinal slope of 0.0004, starting with 0.0003 until station 33.9 km, at CS5, and then got steeper to become 0.0005 up to the end of the reach. The flow in the river reach is slightly decreased by 15% due to irrigation and domestic consumption. Measured discharges at the location of Makhool Dam for the period from Sept 2021 to Feb 2022 were 425, 429, 462, 425, 442, and 470 on 9 Sept 2021, 21 Oct 2021, 18 Nov 2021, 29 Dec 2021, 27 Jan 2022 and 25 Feb 2022, respectively. They slightly fluctuated between 470 m³/s and 425 m³/s. The measured discharges are significantly less than the maximum (11571m³/s), which is recorded at the Baiji Hydrological Station by IMoWR on 12 April 2019, and greater than the minimum (286 m³/s), which is recorded at the same station by IMoWR on 8 July 2021. However, during the filed investigation period there was no high flow.

3.2. Delineation of River Reach and Change Detection

Results of delineating the river reach by using the satellite-based indices (NDVI and NDWI) for the considered years (1975, 1984, 1988, 1995, 2000, 2005, 2010, 2015, 2019, and 2021) for the wet (represented by April) and dry (represented by September, except for 1975 where it was for July) seasons are shown in Figures A1 to A20 in Appendix I.

The results show many mild sinuosities in the river reach with many braided parts with the emergence and growth of some islands and bars. In addition to the disappearance of some branches permanently. Also, most of the reach parts have mild slope flood plains, which are not submerged by water except during periods of high floods. Also, it was observed that the water usually flows in deep braided streams, rather than in a wide section of the river. In the distance extending from the location of Makhool Dam to the Fatha Village, Makhool Mountains Series bounded the right side of the river reach. This makes the right bank of the river has a steep side slope and the right flood plain has a short length. However, the side slope of the left flood plain is mild and this plain is long. At the Fatha, Makhool Mountains Series crosses the river reach and the main channel of the river became narrow and deep without appreciable flood plains. After the Fatha, Makhool Mountains Series moves eastward away from the river basin, the river basin widens again, and the lateral slopes of both flood plains become mild. The river's reach splits back into many braided channels, so it is difficult to recognize the main channel. This part is characterized by the abundance of islands and bars, and most of them are covered with grass and shrubs. Most of the islands are characterized by low altitudes, which makes them submerged in water during flood periods.

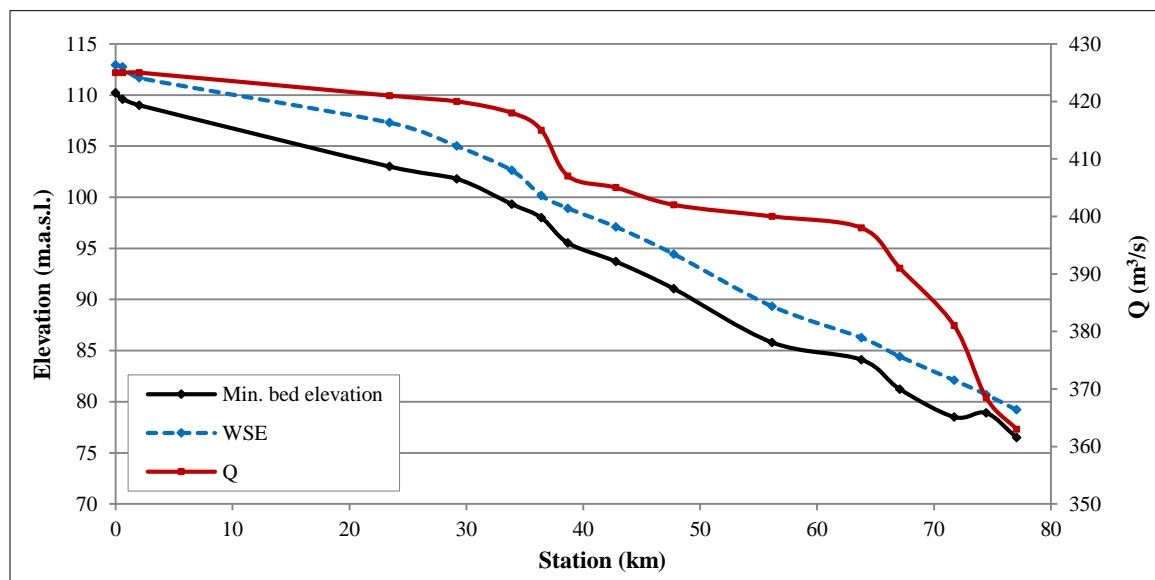


Figure 4. Profile of Makhool-Tikrit Reach with measured Q and WSE on 9 to 10 Sep. 2021

According to the results of satellite-based delineation of the considered reach, a comparison of the main channel path before (1975) and after (1994) the construction of Mosul Dam for the wet season (represented by April) and dry season (represented by September, except for 1975 where it was for July) (Figures 5-a and 5-b), which were low flow years, shows that some of the shallow channels were starting to fading out due to less frequency of high flow, growing of some island, moving of some bends downstream and destruction of some deep channels of the river, as well as some change in the path of the main channel. The rate of changing parts of the reach is approximately 11% of the total length. However, the long-term comparison for the period 1975-2021 in wet and dry seasons (Figures 5-c and 5-d), which are low flow years, indicates the continuation of fewer changes in some of the same parts as well as some others, with a rate of approximately 14% of the total length. To evaluate the state of the reach for high flow conditions, the determined river layouts for the flooded years 1988 and 2019 in wet and dry seasons were compared (Figures 5-e and 5-f). This comparison illustrates the locations of growing islands and bars as well as the change in the extent of flood plains across the river width. However, a comparison of the reach layout in the wet season with this in the dry season for these two years (Figures 5-g and 5-h) pointed out the same changes that were obtained in the long-term comparison (Figures 5-g and 5-h).

Based on the results of reach delineation for the highest flow in the wet season (Apr 1988), the river boundary was specified (Figure 7). Based on this boundary, the determined total area of the river reach basin is 120.83 km². Thus, the water area rates of the main channel to flood plain for the period 1975-2021 were computed (Figure 6). These rates indicated a decrease in the areas of the watercourse for the wet and dry seasons by 18% and 33%, respectively. This can be attributed to the growth of islands and bars in the watercourse as a result of the decrease in the discharges and frequency of high flood waves after the construction of the Mosul Dam. Also, the fact that the percentage of decrease

in the areas of the watercourse in the dry season is higher than that of the wet season shows that the altitudes of islands and bars growing in the river course are not high and remain within the limits of water levels during the dry seasons or slightly higher so that most of these islands and bars are submerged with the increase in water levels during the wet season.

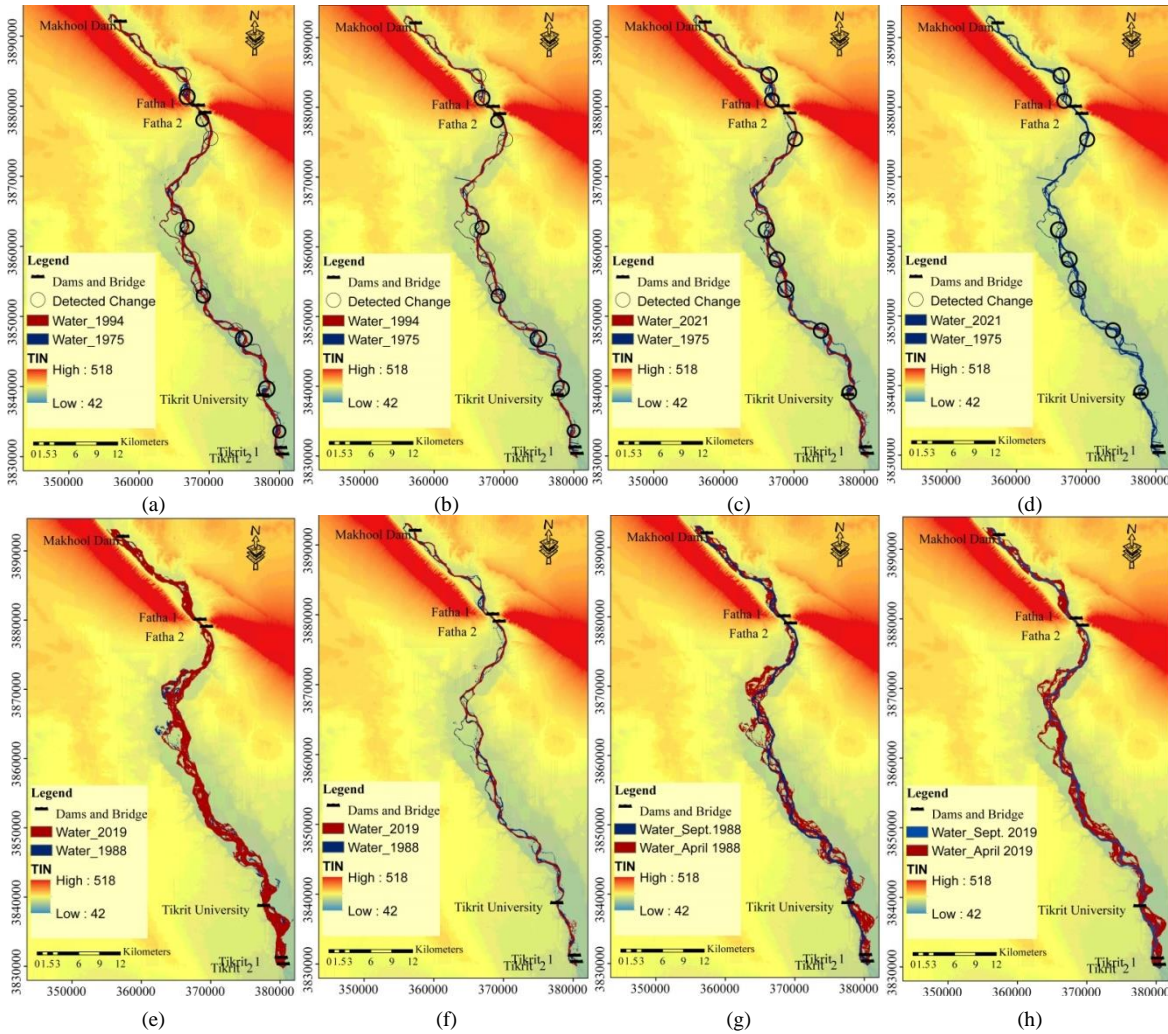


Figure 5. Comparison of the channel Path: (a) April of 1994 and 1975; (b) Sept. 1994 and July 1975; (c) April of 2021 and 1975; (d) Sept. 2021 and July 1975; (e) April of 1988 and 2019; (f) Sept. of 1988 and 2019; (g) April and Sept. of 1988; (h) April and Sept.

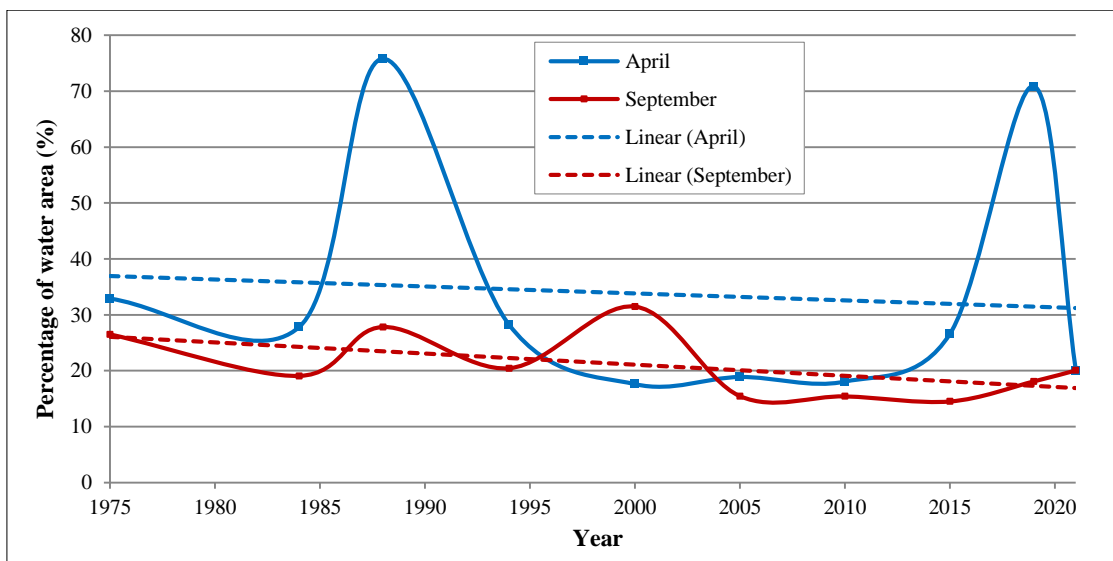


Figure 6. Percentage of the watercourse area

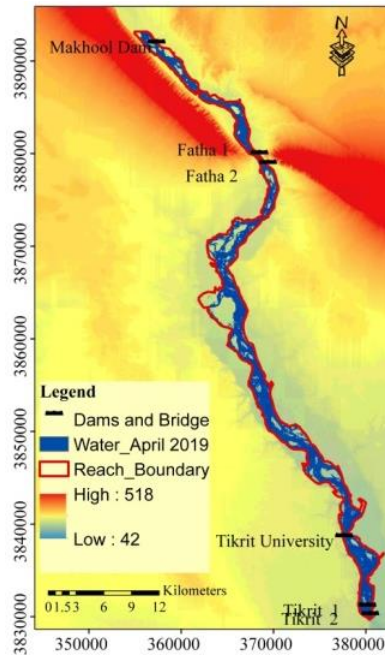


Figure 7. The boundary of the river reach basin

3.3. River Channel Aspects

Based on the results of surveyed 15 CSs (Figure 3) and the satellite indices-based delineation of river reach for Sept 2021 and Apr 2019, the planform of the considered river reach was analyzed by adopting sinuosity indexes. The layout of the river indicates nine meandered segments (Figure 8). The obtained measures of the sinuosity and braiding, which are CL, AL, VL, A_b , A_t , N_b , and L_b , by using the Arc GIS tools, and the computed sinuosity and braiding indices, which are CI, VI, HIS, TSI, SSI, BRI, and MBI, based on Khan et al. (2018) [3], Gemanoski and Schumm (1993) [51] and Sarma and Acharjee (2018) [54], are presented in Table 2. The obtained values of sinuosity indices for reach segments were less than 1.5, except that for the fifth segment where it was greater than 1.5. This indicated that reach segments were sinuous except the fifth segment, which was meandering. However, computed sinuosity indices along the total length of the Makhool-Tikrit reach were less than 1.5 (Table 3). Thus, the considered reach is sinuous. This indicates that there is no high degree of sinuosity because of the absence of obstacles and topographic, geological, or hydraulic factors that lead to large deviations in the directions of flow within a short and long length of the river reach.

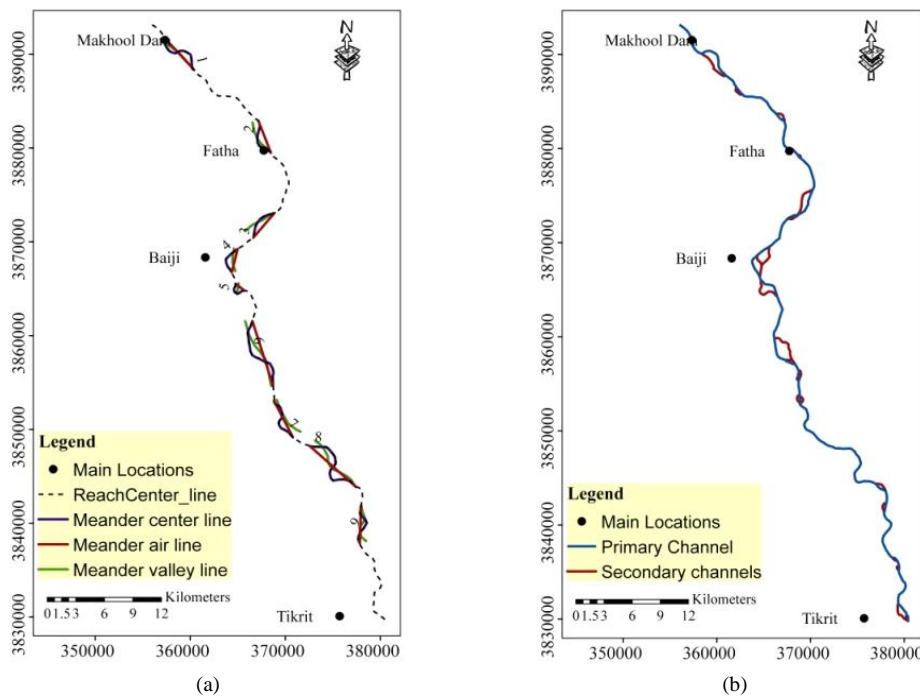


Figure 6. The layout of the river reach for Sept 2021 with sinuosity and measures of meander intensity variables: (a) Meander variables; (b) primary and secondary channels

Table 2. Measures of the sinuosity and the computed sinuosity indices in nine meandered segments of the river reach

Sub-reach No	CL	VL	AL	CI	VI	HSI	TSI	SSI	Sinuosity Degree
1	5829.1	4852.0	4739.2	1.2	1.0	0.9	0.10	1.2	Sinuosity
2	4261.3	3873.6	3660.7	1.1	1.1	0.7	0.35	1.1	Sinuosity
3	3858.4	3716.2	3461.9	1.1	1.1	0.4	0.64	1.0	Sinuosity
4	3229.2	2451.7	2573.8	1.3	1.0	1.2	-0.19	1.3	Sinuosity
5	2079.0	1162.0	1152.0	1.8	1.0	1.0	0.01	1.8	Meandering (CI and SSI>1.5)
6	8338.1	7566.6	7224.4	1.2	1.1	0.7	0.31	1.1	Sinuosity
7	5059.7	4364.2	4388.4	1.2	1.0	1.0	-0.04	1.2	Sinuosity
8	8673.9	6873.2	6514.8	1.3	1.1	0.8	0.17	1.3	Sinuosity
9	4527.0	4151.1	3972.2	1.1	1.1	0.7	0.32	1.1	Sinuosity

The computed braiding indices were less than 1 (Table 3). Therefore, the studied reach is sinuous with alternating bars. Moreover, evaluation of islands and bars areas and the ratio of length to width (Figure 9) shows that most of the islands and bars (85%) have an area of less than 1 km², where the maximum is 3.94 km² and the minimum is 0.001 km².

Table 3. Measures of the sinuosity and the computed sinuosity indices of the river reach

Aspect	Measures and computed Indices	Value	
Sinuosity	Measures	Channel Length (CL)	88.2 km
		Valley Length (VL)	78.3 km
		Air Length (AL)	6.8 km
	Indices	Channel Index (CI)	1.3
		Valley Index (VI)	1.2
		Hydraulic Sinuosity Index (HSI)	0.5
		Topographic Sinuosity Index (TSI)	0.5
Braiding	Indices	Standard Sinuosity Index (SSI)	1.1
	Measures	Total area of the islands and bars (Ab)	56.3 km
		Total channel area (At)	240.1 km
		Number of bars and islands (Nb)	35
		Valley Length (VL)	78.3 km
		Sum of bars and island length (Lb)	22.7
	Indices	Modified the braid index (MBI _B)	0.6
	Braiding Ratio Index (BR)	0.2	

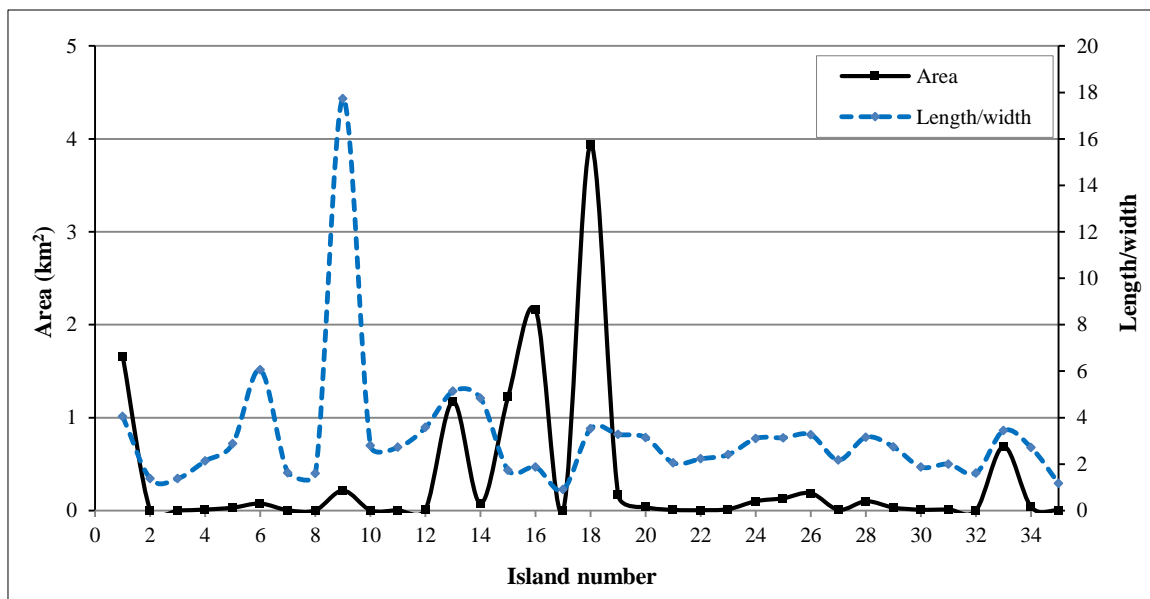


Figure 7. Area and length/width of the island within Makhool-Tikrit Reach

3.4. River Bed Material

Based on the laboratory tests of the collected samples for the 15 CSs, the grain size distribution of surface and subsurface bed material are determined (Figure 10). The specific density of surface and subsurface bed material has a range between 2.43 and 2.82 g/cm³ and an average of 2.59 g/cm³. The particle sizes of 16%, 50%, and 84% finer were determined. According to Wnetworth (1992) [67] grain size of coarse gravel and medium gravel were the dominant particle sizes along the considered river reach. The geometric standard deviation can be considered an indicator of the homogeneity of the bed material [13, 15]. Variation of D₅₀ (mm) for the surface and subsurface layers along the studied reach (Figure 11) has a negative trend towards the end of the studied reach. However, the variation trend of the surface layer is steeper than this of the subsurface. The classification of these particles (Figure 12) is based on Zingg [66]. Zingg develop a classification based on the 3 axes' relation, in this way it is easy to find out the main form of the particles as disks, spherical, blades, and rods. Three mutually perpendicular axes of the surface layer of bed material particles, the longest (a-axis), the intermediate (b-axis), and the shortest (c-axis) were measured. Analysis of the Makhool-Tikrit Reach components of bed material shows that the disc particles have the highest percentage with an average rate of 49%, then the blade of 21%, spherical of 16%, and cylindrical particles of 13%. These results agree with that obtained in Mosel City by Othman & Deguan (2004) [13].

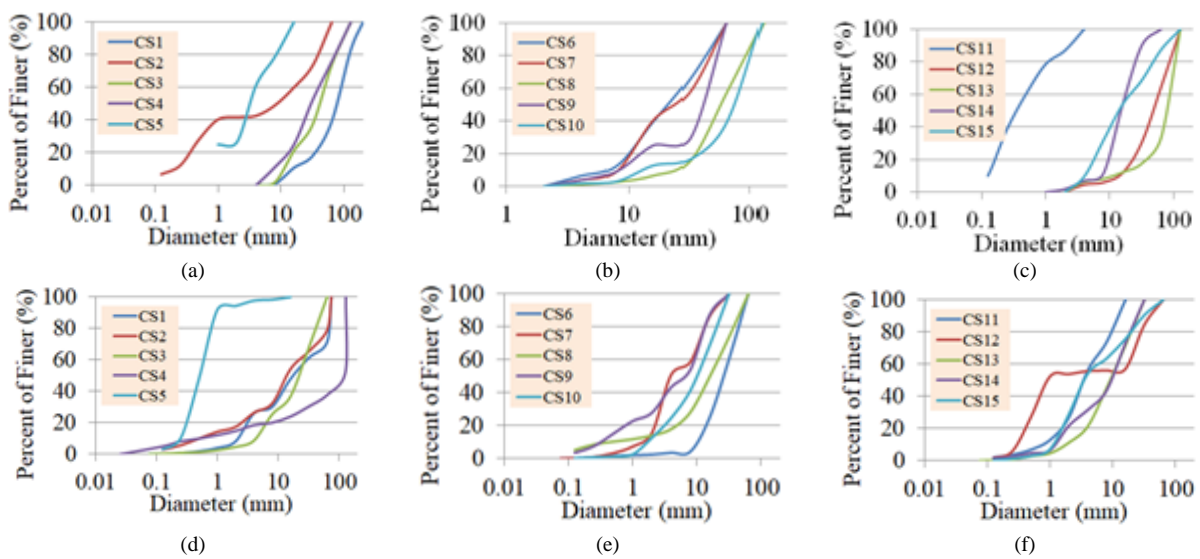


Figure 8. Grain Size Distribution of Bed Material along Makhool-Tikrit reach: (a)-(c) for surface layer of CS1 to CS5, CS6 to CS10 CS11 to CS15 respectively; (d)-(f) for subsurface layer of CS1 to CS5, CS6 to CS10 CS11 to CS15 respectively

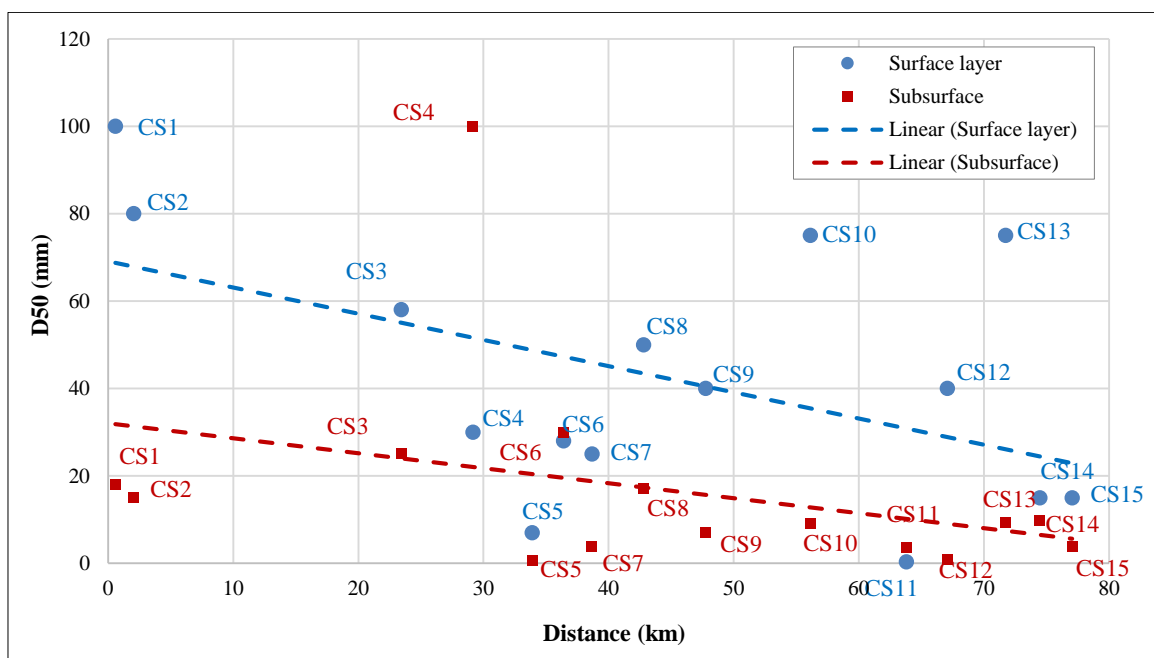


Figure 9. Variation of D₅₀ (mm) of the surface layer for the study reach

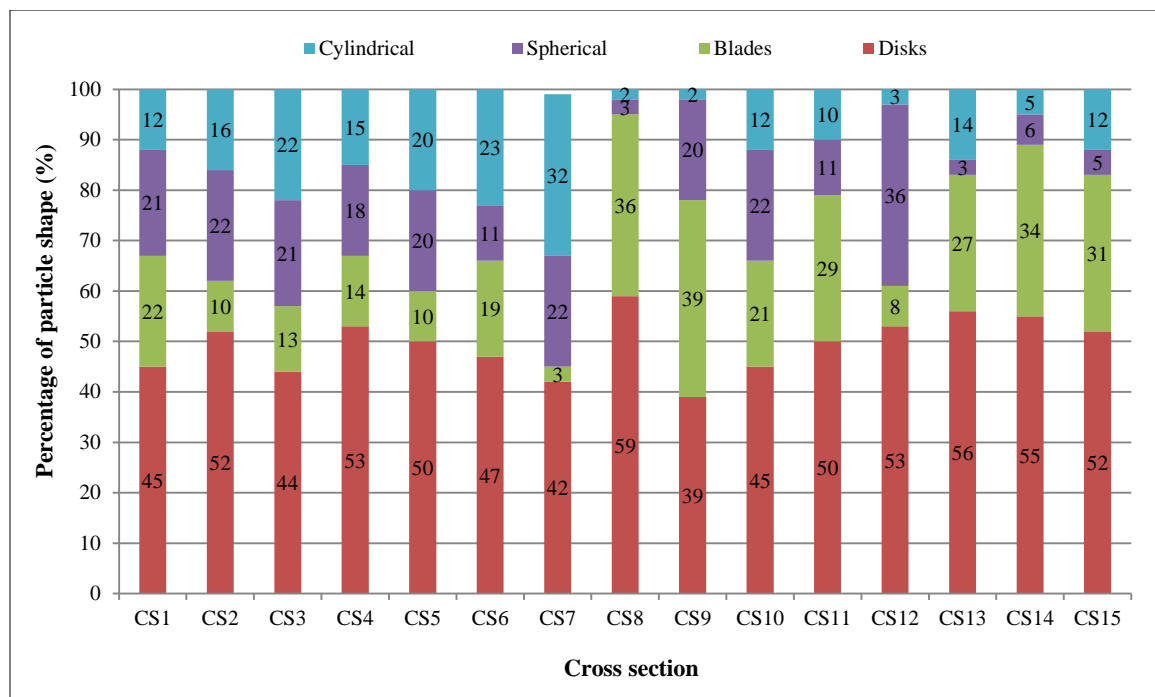


Figure 10. Classification of particle shape for the surface layers

In recent years, in conjunction with the sharp decline in Tigris River discharges, many researches and studies that dealt with morphological modeling and sediment transport were carried out on the Tigris River. These studies required accurate knowledge of the nature and physical properties of the bed material, which prompted some authors to conduct field investigations for bed materials [13, 15-18, 22], as well as this study. Most of those researchers studied the morphology of many reaches in the Tigris River (the Makhool-Tikrit reach was not included) through analysis of the bed material of these reaches. Othman & Deguan (2004) [13] and Othman et al. (2012) [15] analyzed the bed material of the Tigris River in Mosul City, and the analysis results showed that the dominant component of bed material is very coarse gravel to coarse gravel. In Baghdad, Al-Ansari et al. (2015) [16] found that the dominant component of bed material is fine sand. Whereas, in Kut City, most of the bed material is fine sand. Whereas, the average D_{50} in Amara was 0.16 mm [22]. However, in this paper, the analysis results of bed materials show that the main component is the medium gravel.

4. Conclusion

This paper deals with the investigation of the morphological characteristics of the Makhool-Tikrit Reach of the Tigris River. For this purpose, the topographical and planform characteristics of this reach were determined and evaluated. This assessment was conducted by applying the methodology of field investigations of the river topography and bed materials for the year 2021. In addition, remote sensing techniques were used to delineate the layout, analyze the planform, and perform change detection of the reach via applying the satellite-based indices of land cover classification on the satellite images of the years 1975, 1984, 1988, 1994, 2000, 2005, 2010, 2015, 2019, and 2021 for the wet and dry periods for each year.

The main findings indicated a significant variation in the river geometry along the river reach. The reach has a steep bed slope of 0.0004, where the minimum bed level decreased by 33 m to be 76.5 m.a.s.l. in Tikrit City. The first quarter of the reach has high banks with a steep lateral slope on both sides. Thus, this part of the reach safely controls and conveys the flood wave and prevents the flood risk. However, other parts of the reach are characterized by extreme flatness, which exposes the vicinity to flood risk. Most of the river reach has a mild sinuosity with alternating bars, as well as the emergence and growth of several islands and bars, and the disappearance of many secondary channels in the reach basin. Furthermore, most of the reach parts have mild slope flood plains. There are many islands in the river. Most of these islands (85%) have an area of less than 1 km². Also, most of these islands (88%) have an elongated shape in the direction of flow. For more than half of the islands (59%), the length is greater than twice the width. This indicates that the reason for the island's formation is sedimentation and not due to the nature of the geological formation of the river basin. Most of the growing islands have low altitudes, which makes them submerged in water during flood periods. The short-term comparison of the main channel path before and after the construction of Mosul Dam, in 1975 and 1994, respectively, shows that some of the shallow channels were starting to fade out due to less frequency of high flow, the growth of some islands, the moving of some bends downstream, and the destruction of some deep channels of the river, as well as some change in the path of the main channel. The rate of change of parts of

the reach is approximately 11% of the total length. However, the long-term comparison for the period 1975–2021 indicates the continuation of fewer changes in some of the same parts as well as some others, with a rate of approximately 14% of the total length. Moreover, evaluation of the bed material shows that the dominant particle sizes along the considered river reach are coarse and medium gravel. Also, it is found that the surface and subsurface layers have coarser grain sizes in most of the river's reach. Furthermore, it is observed that the dominant particle shape in the surface and subsurface layer is the disc particles, followed by the blade, cylindrical, and spherical particles. The conducted fieldwork and the applied methodology contribute to supporting efforts to add knowledge worldwide about uninvestigated rivers.

5. Declarations

5.1. Author Contributions

Conceptualization, A.H.N. and A.S.A.; methodology, A.H.N. and J.S.M.; software, A.H.N.; validation, A.H.N., and J.S.M. ; formal analysis, A.H.N. ; investigation, A.H.N. and J.S.M.; resources, A.H.N.; data curation, A.H.N.; writing—original draft preparation, A.H.N.; writing—review and editing, A.S.A. and J.S.M.; visualization, A.H.N.; supervision, A.S.A. and J.S.M.; funding acquisition, A.H.N. All authors have read and agreed to the published version of the manuscript.

5.2. Data Availability Statement

The data presented in this study are available on request from the corresponding author. However, IMoWR (1985) [Fatha Dam Project, Study of Operation of Fatha Dam and Lake Tharthar and Optimization of Dam Height (Volume 1)] is an unpublished report, available at the library of MoWR, Iraq. It can be received upon an official request. Also, IMoWR (2021) [Documented Data] is unpublished data, available at the Salahaldin Directorate of Water Resources, MoWR, Iraq. It can be received upon an official request.

5.3. Funding

This research was funded by the Ministry of Water Resources, Iraq, Contract No. 1/Study/Dams/2021.

5.4. Acknowledgements

The authors would like to thank the State Commission of Dams and Reservoirs (SCDR) of the Ministry of Water Resources (MoWR), Iraq, for their financial and material support. They also express deep gratitude to the head and staff of the Directorate of Water Resources in Salahaldin Province, Iraq, for their support in the field works. The authors are also grateful to the technical and faculty staff of the Civil Engineering Department at the University of Technology, Baghdad, Iraq, for their valuable support and scientific assistance.

5.5. Conflicts of Interest

The authors declare no conflict of interest.

6. References

- [1] Bollati, I. M., Pellegrini, L., Rinaldi, M., Duci, G., & Pelfini, M. (2014). Reach-scale morphological adjustments and stages of channel evolution: The case of the Trebbia River (northern Italy). *Geomorphology*, 221, 176–186. doi:10.1016/j.geomorph.2014.06.007.
- [2] Intergovernmental Panel on Climate Change. (2014). *Climate change 2013: The physical science basis*. Cambridge University Press, Cambridge, United Kingdom. doi:10.1017/CBO9781107415324.
- [3] Khan, A., Rao, L. A. K., Yunus, A. P., & Govil, H. (2018). Characterization of channel planform features and sinuosity indices in parts of Yamuna River flood plain using remote sensing and GIS techniques. *Arabian Journal of Geosciences*, 11(17). doi:10.1007/s12517-018-3876-9.
- [4] Spada, D., Molinari, P., Bertoldi, W., Vitti, A., & Zolezzi, G. (2018). Multi-temporal image analysis for fluvial morphological characterization with application to Albanian rivers. *ISPRS International Journal of Geo-Information*, 7(8), 314. doi:10.3390/ijgi7080314.
- [5] Caskey, S. T., Blaschak, T. S., Wohl, E., Schnackenberg, E., Merritt, D. M., & Dwire, K. A. (2015). Downstream effects of stream flow diversion on channel characteristics and riparian vegetation in the Colorado Rocky Mountains, USA. *Earth Surface Processes and Landforms*, 40(5), 586–598. doi:10.1002/esp.3651.
- [6] Rhoads, B. L., Lewis, Q. W., & Andresen, W. (2016). Historical changes in channel network extent and channel planform in an intensively managed landscape: Natural versus human-induced effects. *Geomorphology*, 252, 17–31. doi:10.1016/j.geomorph.2015.04.021.

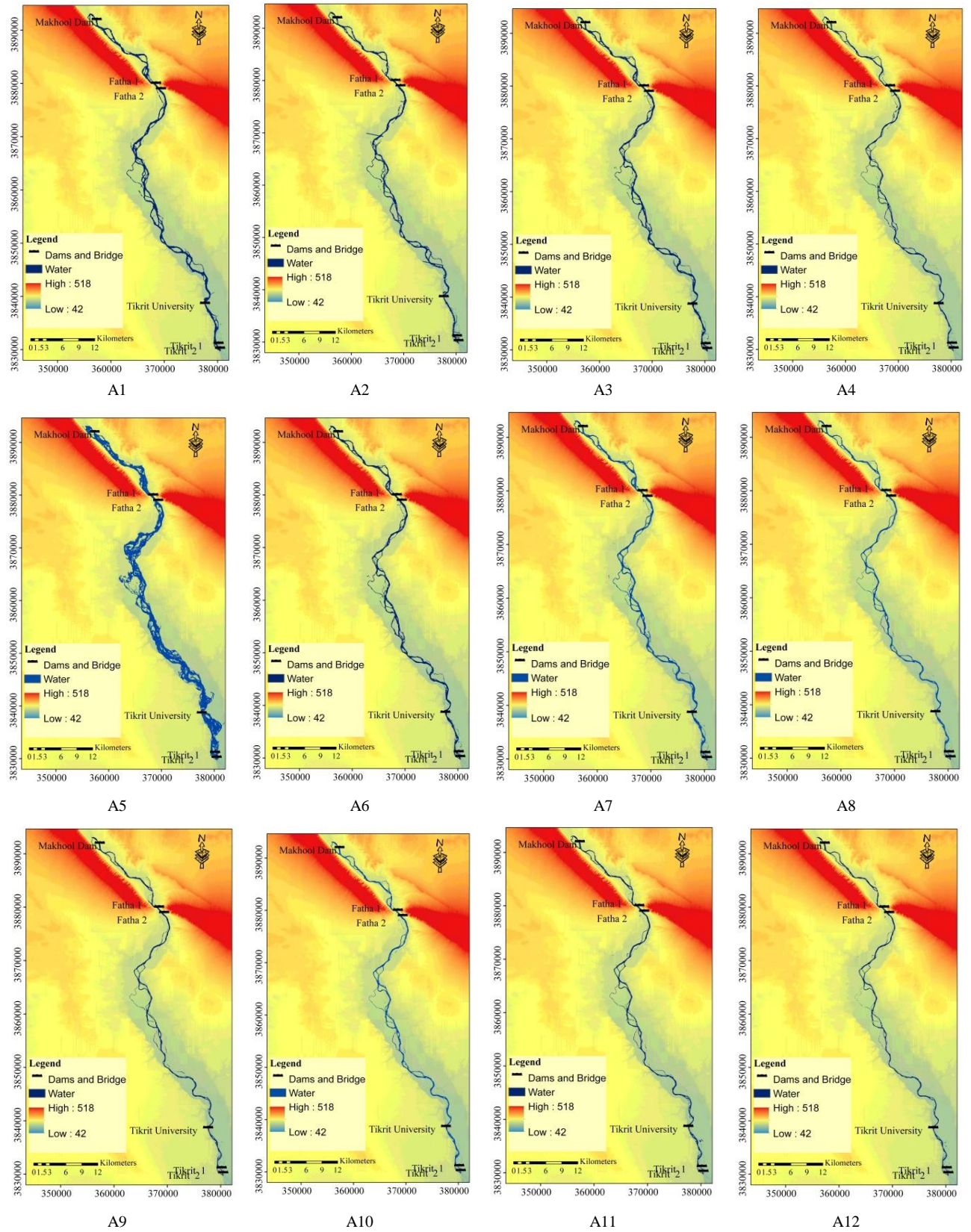
- [7] Yousefi, S., Mirzaee, S., Keesstra, S., Surian, N., Pourghasemi, H. R., Zakizadeh, H. R., & Tabibian, S. (2018). Effects of an extreme flood on river morphology (case study: Karoon River, Iran). *Geomorphology*, 304, 30–39. doi:10.1016/j.geomorph.2017.12.034.
- [8] Boota, M. W., Yan, C., Idrees, M. B., Li, Z., Soomro, S. E. H., Dou, M., Zohaib, M., & Yousaf, A. (2021). Assessment of the morphological trends and sediment dynamics in the Indus River, Pakistan. *Journal of Water and Climate Change*, 12(7), 3082–3098. doi:10.2166/wcc.2021.125.
- [9] Pappas, O. A., Anantrasirichai, N., Achim, A. M., & Adams, B. A. (2021). River Planform Extraction from High-Resolution SAR Images via Generalized Gamma Distribution Superpixel Classification. *IEEE Transactions on Geoscience and Remote Sensing*, 59(5), 3942–3955. doi:10.1109/TGRS.2020.3011209.
- [10] Lin, C. P., Wang, Y. M., Tfwala, S. S., & Chen, C. N. (2014). The variation of riverbed material due to tropical storms in Shi-Wen River, Taiwan. *The Scientific World Journal*, 2014, 1–12. doi:10.1155/2014/580936.
- [11] Ermilov, A. A., Baranya, S., & Török, G. T. (2020). Image-based bed material mapping of a large river. *Water (Switzerland)*, 12(3), 916. doi:10.3390/w12030916.
- [12] Al-Ansari, N. (2020). Water Resources of Iraq. *Journal of Earth Sciences and Geotechnical Engineering*, 15–34. doi:10.47260/jesge/1122.
- [13] Othman, K., & Deguan, W. (2004). Characteristics of Tigris River Bed at Mosul City, Iraq. *Journal of Lake Sciences*, 16(Z1), 61–70. doi:10.18307/2004.sup08.
- [14] Nama, A. H. (2011). Estimating the Sediment Transport Capacity of Tigris River within Al Mosul City. *Journal of Engineering*, 17(3), 473–485.
- [15] Othman, K., Bilal, A. A., & Sulaman, Y. I. (2012). Morphologic Characteristics of Tigris River with at Mosul City. *Tikrit Journal of Engineering Sciences*, 19(3), 36–54. doi:10.25130/tjes.19.3.12.
- [16] Al-Ansari, N., Ali, A. A., Al-Suhail, Q., & Knutsson, S. (2015). Flow of River Tigris and its Effect on the Bed Sediment within Baghdad, Iraq. *Open Engineering*, 5(1), 465–477. doi:10.1515/eng-2015-0054.
- [17] Ali, A. (2016). Three dimensional hydro-morphological modeling of Tigris River. PhD Thesis, Luleå University of Technology, Luleå, Sweden.
- [18] Shamkhi, M. S., & Attab, Z. S. (2019). Characteristics of Tigris River bed material at 67 Km Downstream Kut Barrage. *Wasit Journal of Engineering Sciences*, 7(1), 54–61. doi:10.31185/ejuow.vol7.iss1.114.
- [19] AL-Thamiry, H. A. K., & AbdulAzeez, T. M. (2017). Two-Dimensional mathematical model to study erosion problem of Tigris River banks at Nu'maniyah. *Journal of Engineering*, 23(1), 112-135.
- [20] Abbas, M. s., & Azzubaidi, R. Z. (2020). Current and Modified Flood Discharge Capacity of a Reach of Tigris River between Kut and Amarah Barrages. *Journal of Engineering*, 26(2), 129–143. doi:10.31026/j.eng.2020.02.10.
- [21] Asaad, B. I., & Abed, B. S. (2020). Flow Characteristics Of Tigris River Within Baghdad City During Drought. *Journal of Engineering*, 26(3), 77–92. doi:10.31026/j.eng.2020.03.07.
- [22] Ismaeel, A., Abbas, S., & Al-Rekabi, W. (2021). Numerical 3D Model of Suspended Sediment Transport Downstream Al-Amarah Barrage, Iraq. *Basrah Journal for Engineering Science*, 21(3), 73–80. doi:10.33971/bjes.21.3.9.
- [23] Buscombe, D., Masselink, G., & Rubin, D. M. (2009). Granular Properties from Digital Images of Sediment: Implications for Coastal Sediment Transport Modelling. *Coastal Engineering*, 1625–1637. doi:10.1142/9789814277426_0135.
- [24] Graham, D. J., Rollet, A.-J., Rice, S. P., & Piégay, H. (2012). Conversions of Surface Grain-Size Samples Collected and Recorded Using Different Procedures. *Journal of Hydraulic Engineering*, 138(10), 839–849. doi:10.1061/(asce)hy.1943-7900.0000595.
- [25] Suwarno, I., Ma'arif, A., Maharani Raharja, N., Nurjanah, A., Ikhsan, J., & Mutiarin, D. (2021). IoT-based Lava Flood Early Warning System with Rainfall Intensity Monitoring and Disaster Communication Technology. *Emerging Science Journal*, 4, 154–166. doi:10.28991/esj-2021-sp1-011.
- [26] Takechi, H., Aragaki, S., & Irie, M. (2021). Differentiation of river sediments fractions in uav aerial images by convolution neural network. *Remote Sensing*, 13(16), 3188. doi:10.3390/rs13163188.
- [27] Hossain, M. A., Gan, T. Y., & Baki, A. B. M. (2013). Assessing morphological changes of the Ganges River using satellite images. *Quaternary International*, 304, 142–155. doi:10.1016/j.quaint.2013.03.028.
- [28] Adib, A., Foladfar, H., & Roozy, A. (2016). Role of construction of large dams on river morphology (case study: the Karkheh dam in Iran). *Arabian Journal of Geosciences*, 9(15), 1-16. doi:10.1007/s12517-016-2693-2.

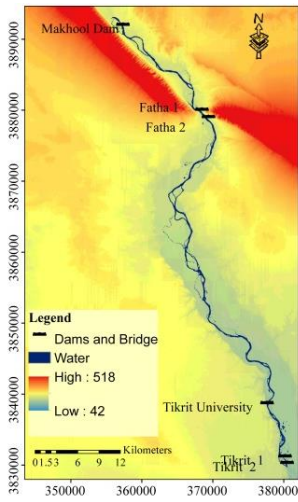
- [29] Pal, R., & Pani, P. (2019). Remote sensing and GIS-based analysis of evolving planform morphology of the middle-lower part of the Ganga River, India. *Egyptian Journal of Remote Sensing and Space Science*, 22(1), 1–10. doi:10.1016/j.ejrs.2018.01.007.
- [30] Boothroyd, R. J., Nones, M., & Guerrero, M. (2021). Deriving Planform Morphology and Vegetation Coverage from Remote Sensing to Support River Management Applications. *Frontiers in Environmental Science*, 9. doi:10.3389/fenvs.2021.657354.
- [31] Prasad, N. (1982). Some aspects of meandering streams of the barakar basin and their sinuosity indexes. *Perspectives in Geomorphology*, 4, 93–102.
- [32] Zámolyi, A., Székely, B., Draganits, E., & Timár, G. (2010). Neotectonic control on river sinuosity at the western margin of the Little Hungarian Plain. *Geomorphology*, 122(3–4), 231–243. doi:10.1016/j.geomorph.2009.06.028.
- [33] Stark, C. P., Barbour, J. R., Hayakawa, Y. S., Hattanji, T., Hovius, N., Chen, H., ... Fukahata, Y. (2010). The Climatic Signature of Incised River Meanders. *Science*, 327(5972), 1497–1501. doi:10.1126/science.1184406.
- [34] Sipos, G., Kiss, T., & Fiala, K. (2007). Morphological alterations due to channelization along the lower Tisza and Maros Rivers (Hungary). *Geografia Fisica e Dinamica Quaternaria*, 30(2), 239–247.
- [35] Chabuk, A., Al-Madhloom, Q., Al-Maliki, A., Al-Ansari, N., Hussain, H. M., & Laue, J. (2020). Water quality assessment along Tigris River (Iraq) using water quality index (WQI) and GIS software. *Arabian Journal of Geosciences*, 13(14). doi:10.1007/s12517-020-05575-5.
- [36] Badowi, M. S., Rashid Abood, M., & Saleh, S. A. (2019). Geotechnical properties for sediment of Tigris River reach banks within Tikrit town/ Iraq. *Tikrit Journal of Pure Science*, 24(6), 65. doi:10.25130/j.v24i6.889.
- [37] UN-ESCWA, & BGR. (2013). Inventory of Shared Water Resources in Western Asia. Beirut. United Nations Economic and Social Commission for Western Asia; Bundesanstalt für Geowissenschaften und Rohstoffe. Available online: <https://waterinventory.org/sites/waterinventory.org/files/chapters/00-shared-water-resouces-in-western-asia-web.pdf> (accessed on March 2022).
- [38] Dong, L., Deng, S., & Wang, F. (2020). Some developments and new insights for environmental sustainability and disaster control of tailings dam. *Journal of Cleaner Production*, 269, 122270. doi:10.1016/j.jclepro.2020.122270.
- [39] Shareef, M. E., & Abdulrazzaq, D. G. (2021). River Flood Modelling For Flooding Risk Mitigation in Iraq. *Civil Engineering Journal*, 7(10), 1702–1715. doi:10.28991/cej-2021-03091754.
- [40] Jones, A. F., Brewer, P. A., Johnstone, E., & Macklin, M. G. (2007). High-resolution interpretative geomorphological mapping of river valley environments using airborne LiDAR data. *Earth Surface Processes and Landforms*, 32(10), 1574–1592. doi:10.1002/esp.1505.
- [41] Harmar, O. P., & Clifford, N. J. (2006). Planform dynamics of the Lower Mississippi River. *Earth Surface Processes and Landforms*, 31(7), 825–843. doi:10.1002/esp.1294.
- [42] Winterbottom, S. J. (2000). Medium and short-term channel planform changes on the Rivers Tay and Tummel, Scotland. *Geomorphology*, 34(3–4), 195–208. doi:10.1016/S0169-555X(00)00007-6.
- [43] Sarma, J. N., & Basumallick, S. (1986). Channel Form and Process of the Burhi Dihing River, India. *Geografiska Annaler: Series A, Physical Geography*, 68(4), 373–381. doi:10.1080/04353676.1986.11880187.
- [44] Miller, T. K. (1988). An analysis of the relation between stream channel sinuosity and stream channel gradient. *Computers, Environment and Urban Systems*, 12(3), 197–207. doi:10.1016/0198-9715(88)90022-1.
- [45] Ratzlaff, J. (1991). Sinuosity Components of the Upper Saline River Valley, Western Kansas. *Transactions of the Kansas Academy of Science*, 94(1-2), 46-57. doi:10.2307/3628040.
- [46] Julien, P. Y. (2018). *River mechanics*. Cambridge University Press, Cambridge, United Kingdom. doi:10.1017/9781316107072.
- [47] Ebisemiju, F. S. (1994). The sinuosity of alluvial river channels in the seasonally wet tropical environment: Case study of river Elemi, southwestern Nigeria. *CATENA*, 21(1), 13–25. doi:10.1016/0341-8162(94)90028-0.
- [48] Charlton, R. (2007). *Fundamentals of fluvial geomorphology*. Routledge, London, United Kingdom. doi:10.4324/9780203371084.
- [49] Brice, J. C. (1964). *Channel patterns and terraces of the Loup Rivers in Nebraska*. US Government Printing Office, Washington, United States. doi:10.3133/pp422d.
- [50] Rust, B. R. (1977). A classification of alluvial channel system. *Modern Rivers: Geomorphology and Sedimentation, Fluvial Sedimentology*, 187-198.
- [51] Germanoski, D., & Schumm, S. A. (1993). Changes in braided river morphology resulting from aggradation and degradation. *Journal of Geology*, 101(4), 451–466. doi:10.1086/648239.

- [52] Friend, P. F., & Sinha, R. (1993). Braiding and meandering parameters. *Geological Society Special Publication*, 75(1), 105–111. doi:10.1144/GSL.SP.1993.075.01.05.
- [53] Gil-Guirado, S., Pérez-Morales, A., Pino, D., Peña, J. C., & Martínez, F. L. (2022). Flood impact on the Spanish Mediterranean coast since 1960 based on the prevailing synoptic patterns. *Science of the Total Environment*, 807, 150777. doi:10.1016/j.scitotenv.2021.150777.
- [54] Sarma, J. N., & Acharjee, S. (2018). A study on variation in channel width and braiding intensity of the Brahmaputra River in Assam, India. *Geosciences (Switzerland)*, 8(9), 343. doi:10.3390/geosciences8090343.
- [55] Rinaldi, M., Surian, N., Comiti, F., & Bussetini, M. (2011). Guidebook for the evaluation of stream morphological conditions by the Morphological Quality Index (IQM). Higher Institute for Environmental Protection and Research (ISPRA), Rome, Italy. Available online: <https://www.isprambiente.gov.it/en/publications/handbooks-and-guidelines/guidebook-for-the-evaluation-of-stream-1> (accessed on March 2022).
- [56] Huang, S., Tang, L., Hupy, J. P., Wang, Y., & Shao, G. (2021). A commentary review on the use of normalized difference vegetation index (NDVI) in the era of popular remote sensing. *Journal of Forestry Research*, 32(1), 1–6. doi:10.1007/s11676-020-01155-1.
- [57] McFeeters, S. K. (1996). The use of the Normalized Difference Water Index (NDWI) in the delineation of open water features. *International Journal of Remote Sensing*, 17(7), 1425–1432. doi:10.1080/01431169608948714.
- [58] Anyamba, A., Tucker, C. J., & Eastman, J. R. (2001). NDVI anomaly patterns over Africa during the 1997/98 ENSO warm event. *International Journal of Remote Sensing*, 22(10), 1847–1859. doi:10.1080/01431160010029156.
- [59] Partow, H., & Jaquet, J. (2006). Iraqi Marshlands Observation System. UNEP Technical Report. United Nations Environmental Program (UNEP), Nairobi, Kenya, 74.
- [60] Fisher, A., Flood, N., & Danaher, T. (2016). Comparing Landsat water index methods for automated water classification in eastern Australia. *Remote Sensing of Environment*, 175, 167–182. doi:10.1016/j.rse.2015.12.055.
- [61] Ji, L., Zhang, L., & Wylie, B. (2009). Analysis of dynamic thresholds for the normalized difference water index. *Photogrammetric Engineering and Remote Sensing*, 75(11), 1307–1317. doi:10.14358/PERS.75.11.1307.
- [62] Issa, I. E., Al-Ansari, N. A., Sherwany, G., & Knutsson, S. (2013). Trends and future challenges of water resources in the Tigris–Euphrates Rivers basin in Iraq. *Hydrology and Earth System Sciences Discussions*, 10, 14617–14644. doi:10.5194/hessd-10-14617-2013.
- [63] Diplas, P., & Sutherland, A. J. (1988). Sampling Techniques for Gravel Sized Sediments. *Journal of Hydraulic Engineering*, 114(5), 484–501. doi:10.1061/(asce)0733-9429(1988)114:5(484).
- [64] Fripp, J. B., & Diplas, P. (1993). Surface Sampling in Gravel Streams. *Journal of Hydraulic Engineering*, 119(4), 473–490. doi:10.1061/(asce)0733-9429(1993)119:4(473).
- [65] Laronne, J. B., Reid, I., Yitshak, Y., & Frostick, L. E. (1994). The non-layering of gravel streambeds under ephemeral flood regimes. *Journal of Hydrology*, 159(1–4), 353–363. doi:10.1016/0022-1694(94)90266-6.
- [66] W. C. Krumbein. (1941). Measurement and Geological Significance of Shape and Roundness of Sedimentary Particles. *SEPM Journal of Sedimentary Research*, Volume 11. doi:10.1306/d42690f3-2b26-11d7-8648000102c1865d.
- [67] Wentworth, C. K. (1922). A Scale of Grade and Class Terms for Clastic Sediments. *The Journal of Geology*, 30(5), 377–392. doi:10.1086/622910.

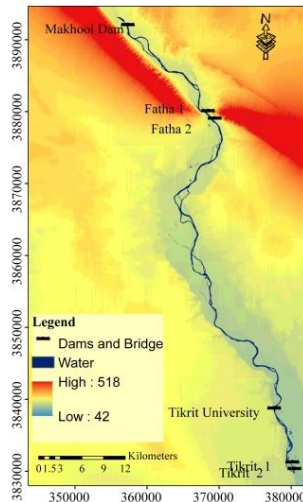
Appendix I

Satellite-based delineation of the Makhool-Tikrit Reach.

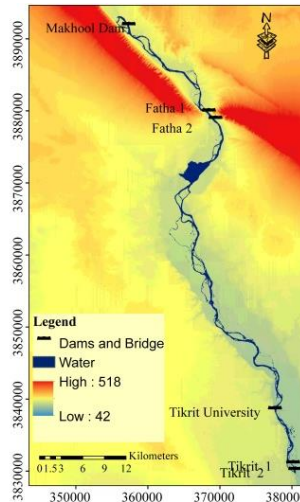




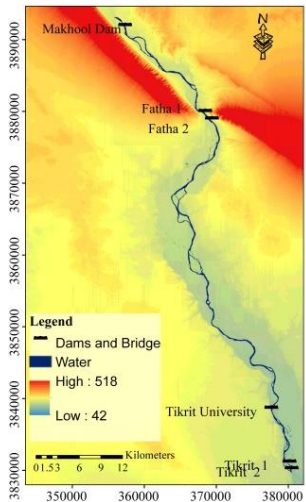
A13



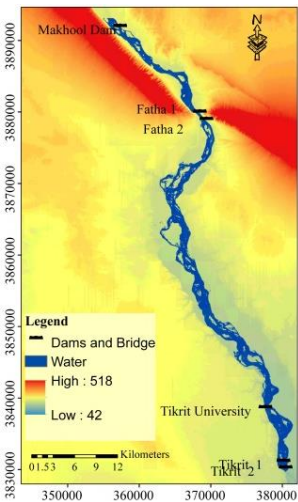
A14



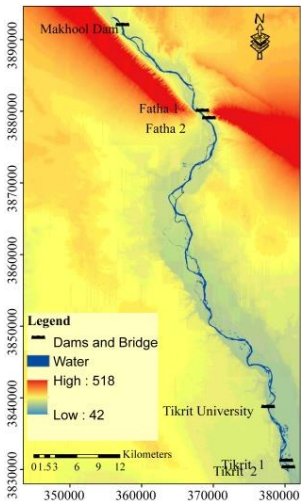
A15



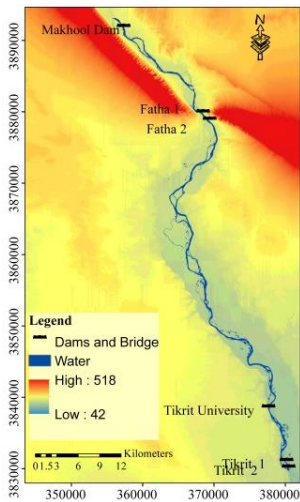
A16



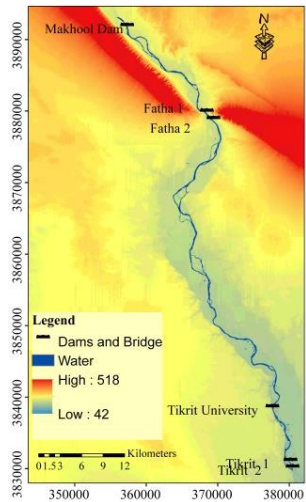
A17



A18



A19



A20